Nanoscale

PAPER

Cite this: *Nanoscale*, 2014, **6**, 2328

Enrichment of large-diameter semiconducting SWCNTs by polyfluorene extraction for high network density thin film transistors†

Jianfu Ding,*[a] Zhao Li,[a] Jacques Lefebvre,[b] Fuyong Cheng,[c] Girjesh Dubey,‡[c] Shan Zou,[d] Paul Finnie,[b] Amy Hrdina,[c] Ludmila Scoles,[e] Gregory P. Lopinski,[d] Christopher T. Kingston,[c] Benoit Simard[c] and Patrick R. L. Malenfant*[b]

A systematic study on the use of 9,9-dialkylfluorene homopolymers (PFs) for large-diameter semiconducting (sc-) single-walled carbon nanotube (SWCNT) enrichment is the focus of this report. The enrichment is based on a simple three-step extraction process: (1) dispersion of as-produced SWCNTs in a PF solution; (2) centrifugation at a low speed to separate the enriched sc-tubes; (3) filtration to collect the enriched sc-SWCNTs and remove excess polymer. The effect of the extraction conditions on the purity and yield including molecular weight and alkyl side-chain length of the polymers, SWCNT concentration, and polymer/SWCNT ratio have been examined. It was observed that PFs with alkyl chain lengths of C10, C12, C14, and C18, all have an excellent capability to enrich laser-ablation sc-SWCNTs when their molecular weight is larger than ~10 000 Da. More detailed studies were therefore carried out with the C12 polymer, poly(9,9-di-*n*-dodecylfluorene), PFDD. It was found that a high polymer/SWCNT ratio leads to an enhanced yield but a reduced sc-purity. A ratio of 0.5–1.0 gives an excellent sc-purity and a yield of 5–10% in a single extraction as assessed by UV-vis-NIR absorption spectra. The yield can also be promoted by multiple extractions while maintaining high sc-purity. Mechanistic experiments involving time-lapse dispersion studies reveal that m-SWCNTs have a lower propensity to be dispersed, yielding a sc-SWCNT enriched material in the supernatant. Dispersion stability studies with partially enriched sc-SWCNT material further reveal that m-SWCNTs : PFDD complexes will re-aggregate faster than sc-SWCNTs : PFDD complexes, providing further sc-SWCNT enrichment. This result confirms that the enrichment was due to the much tighter bundles in raw materials and the more rapid bundling in dispersion of the m-SWCNTs. The sc-purity is also confirmed by Raman spectroscopy and photoluminescence excitation (PLE) mapping. The latter shows that the enriched sc-SWCNT sample has a narrow chirality and diameter distribution dominated by the (10,9) species with $d = 1.29$ nm. The enriched sc-SWCNTs allow a simple drop-casting method to form a dense nanotube network on SiO_2/Si substrates, leading to thin film transistors (TFTs) with an average mobility of 27 $cm^2\ V^{-1}\ s^{-1}$ and an average on/off current ratio of 1.8×10^6 when considering all 25 devices having 25 μm channel length prepared on a single chip. The results presented herein demonstrate how an easily scalable technique provides large-diameter sc-SWCNTs with high purity, further enabling the best TFT performance reported to date for conjugated polymer enriched sc-SWCNTs.

Received 16th October 2013
Accepted 19th December 2013

DOI: 10.1039/c3nr05511f

www.rsc.org/nanoscale

---

[a] *Security and Disruptive Technologies Portfolio, National Research Council Canada, M-12, 1200 Montreal Road, Ottawa, Ontario, K1A 0R6, Canada. E-mail: jianfu.ding@nrc-cnrc.gc.ca*

[b] *Security and Disruptive Technologies Portfolio, National Research Council Canada, M-50, 1200 Montreal Road, Ottawa, Ontario, K1A 0R6, Canada. E-mail: patrick.malenfant@nrc-cnrc.gc.ca*

[c] *Security and Disruptive Technologies Portfolio, National Research Council Canada, 100 Sussex Drive, Ottawa, Ontario, K1A 0R6, Canada*

[d] *Measurement Science and Standards, 100 Sussex Drive, Ottawa, Ontario, K1A 0R6, Canada*

[e] *Energy, Mining and Environment Portfolio, National Research Council Canada, M-12, 1200 Montreal Road, Ottawa, Ontario, K1A 0R6, Canada*

† Electronic supplementary information (ESI) available: Polymer synthesis and thermal characterization yield and SWCNT concentration measurement, SWCNT content evaluation, and sc-purity assessment. See DOI: 10.1039/c3nr05511f

‡ Current address: Max-Planck-Institute for Solid State Research, Heisenbergstraße 1, 70569, Stuttgart, Germany.

Introduction

Since their discovery in the early 1990's,[1,2] carbon nanotubes (CNT) have attracted tremendous attention due to their outstanding properties such as mechanical strength, flexibility, conductivity as well as optical and electronic properties.[3] CNT materials and related composites are expected to be ideal candidates for various applications including photovoltaic devices,[4–6] thin film transistors,[7,8] printable electronics,[8–11] and sensors.[12–15]

An important class of carbon nanotubes are single-walled carbon nanotubes (SWCNTs). Their optical and electronic properties are dependent on their chiralities, defined by their chiral indices (n, m).[16] When $n = m$, they are "armchair" SWCNTs, being metallic with a zero bandgap. When $n - m = 3i$ and $i \neq 0$, the SWCNTs have a very small bandgap, and are generally considered as metallic. When $n - m = 3i \pm 1$, the SWCNTs are semiconducting. Lastly, the SWCNTs with chiral indices of $(n, 0)$ are referred to as "zig-zag" and they could be either metallic or semiconducting following the above rule.

Several methods can be used to produce SWCNTs which vary in the distribution of chiralities, diameter range, semiconducting/metallic (sc-/m-) content and average length. For example, HiPco and CoMoCat SWCNTs are relatively small in diameter (0.6–1.3 nm), while arc-discharge, laser (laser-ablation)[17] and plasma[18–20] SWCNTs are relatively large (1.0–1.9 nm).[21] In the most common syntheses, SWCNTs are produced as ensemble samples containing both metallic and semiconducting nanotubes with a distribution of chiralities.[22a] They usually contain less than 70% sc-SWCNTs, and only some specific techniques such as CVD (*e.g.* using Cobalt Molybdenum alloy catalyst – CoMoCat), can one obtain a sc-SWCNT content as high as 95% *via* synthesis alone.[22b] For many applications, such as thin film transistors (TFTs), a much higher sc-purity is required and in unique cases, single chirality SWCNTs may be desired.[23,24] Therefore, the sc-purity of the as-prepared SWCNTs has to be promoted by the use of a purification and enrichment process.

Many methods have demonstrated the effective enrichment and isolation of sc-SWCNTs with a high sc-purity as assessed by absorption spectroscopy.[25] Some common methods are density gradient ultracentrifugation (DGU),[26,27] gel chromatography (GC),[28–30] dielectrophoresis[31] and selective extraction by conjugated polymers.[22,32–35] Recently, a method based on the partition of nanotubes into two immiscible aqueous phases by exploiting the subtle differences in hydrophobicity between metallic and semiconductor nanotubes has been reported.[36] Amongst these options, we believe that chromatography, partition separation and conjugated polymer extraction provide a clear path to scalable enrichment of sc-SWCNTs. The relative simplicity of the conjugated polymer extraction process, which generally entails a dispersion followed by a centrifugation step, distinguishes it as a cost-effective method for the isolation of sc-SWCNTs with >99% semiconducting content. The interplay between inter-nanotube interactions and polymer – nanotube binding affords this separation method a high selectivity based on differences in the inherent electronic properties between metallic and semiconducting nanotubes. Furthermore, "wrapping" by the polymer encourages the dispersion of individual SWCNTs and provides a means of separation between m-/sc-nanotubes. This provides extremely high purity of SWCNTs, as will be required, for example, for high frequency logic applications.[30,37,38] In addition, the composition and architecture of the polymer side chains can be adjusted to balance the solubilisation and interaction with the nanotubes to optimize the selectivity. Also, the molecular design of the conjugated polymer main-chain will provide unique interactions with the nanotubes as well as some other desired properties such as controllable decomposability.[39–41] The latter is relevant should complete removal of the polymer post-enrichment be required.

The first disclosure that conjugated polymers could selectively disperse semiconducting SWCNTs and lead to enriched fractions of relevance for thin film transistor fabrication can be found in the patent literature.[42,43] Subsequently, a report by Nicholas demonstrated the exceptional selectivity that could be achieved with polyfluorene derivatives towards specific semiconducting SWCNT chiralities.[22] To date, many homo- and copolymers of phenylenevinylene,[34,44–48] carbazole,[49] thiophene,[32,50] and fluorene,[22,34,51–59] have been investigated, yet in many cases only relatively small diameter SWCNTs could be enriched. For example, poly(3-dodecylthiophene) (P3DDT) displayed a promising result in the separation of HiPCO tubes.[32,33] However we observed that P3DDT had poor capability in separating larger diameter SWCNTs such as the SWCNTs derived by laser ablation or plasma synthesis. It is the larger diameter SWCNTs that are more desirable when trying to minimize contact resistance and to obtain a large mobility in thin film transistors.[53] Similarly, it has been observed that poly(9,9-dioctylfluorene), PFO has a high selectivity in dispersing small-diameter sc-SWCNTs with large chiral angles ($20° \leq \theta \leq 30°$),[23,34,52–58] but not large-diameter SWCNTs. The latter are believed to be difficult to disperse and to enrich owing to the strong interaction between these nanotubes that is associated with the low curvature of the nanotube wall.[60] As a result, co-monomer units have been introduced into the polyfluorene main chain in order to target specific tube chiralities/diameters. They include: phenylene-1,4-diyl,[34] thiophen-2,5-diyl,[57,58] anthracene-9,10-diyl,[52] anthracene-1,5-diyl,[52] naphthalene-1,5-diyl, 2,2-bithiophene-5,5′-diyl,[52,61] and benzo-2,1,3-thiadiazole-4,7-diyl.[34,51,52]

Furthermore, the length of the side alkyl chain of PFs has a significant impact on the enrichment effectiveness.[59,62–66] PFs with 12-carbon side chains showed an improved selectivity towards sc-SWCNTs with larger diameters.[59–63] Successful enrichment with fluorene based homopolymers and copolymers were recently reported for larger diameter SWCNTs with alkyl chains ranging from C12 to C18.[59,67] While several recent reports highlight the isolation of high purity large-diameter sc-SWCNTs using various methods or combinations thereof, only a few reports include the TFT performance of these materials.[43,57,59,60] TFT device performance is an effective way to validate the high sc-purity of enriched sc-SWCNTs when simultaneously considering mobility, on/off current ratio and current density.

Herein, we show that 9,9-dialkylfluorene homopolymers with optimized molecular weight and adequately long alkyl side-chains are highly effective at selectively dispersing large-diameter, laser-derived sc-SWCNTs in toluene. A simple combination of dispersion, centrifugation and filtration steps provided SWCNTs with a sc-purity higher than 99% as assessed by absorption spectroscopy. We also present a mechanistic interpretation of this polymer driven enrichment of sc-SWCNT using time-lapse studies. This process utilizes a conjugated polymer with a simple structure (homopolymer *vs.* copolymer) which will positively affect the cost of this process. Thin film transistor devices utilizing the enriched sc-SWCNTs as the channel semiconductor possess an average mobility of 27 $cm^2 V^{-1} s^{-1}$ and current on/off ratio of 1.8×10^6 when considering all 25 devices with a 25 μm channel length prepared on a single wafer *via* a simple drop-cast protocol and using a parallel plate model for mobility calculation. This is the best TFT performance data reported so far for conjugated polymer enriched large-diameter sc-SWCNTs. The generality of this approach is further evidenced by the successful enrichment and similar device performance for plasma derived SWCNTs, which can be synthesized in kilogram quantities *via* a commercial process.[18–20]

Experimental section

Chemicals

All chemicals and solvents (HPLC grade) were purchased from Sigma-Aldrich and used as received. Poly(9,9-dialkylfluorenes) with C10, C12, C14 and C18 alkyl side-chains were prepared by the Suzuki coupling reactions, as detailed in the ESI.† SWCNT soot was prepared using a laser ablation technique from biochar.[17] Its SWCNT content was estimated to be 53 wt% from the TGA curve of the raw sample, see ESI.† Due to the possible catalytic decomposition of the SWCNTs at temperatures lower than 600 °C, the actual SWCNT content could be slightly higher than this value.[68]

Characterization

Proton nuclear magnetic resonance (^1H NMR) spectra were recorded using a Varian Unity Inova spectrometer at a resonance frequency of 400 MHz. The chemical shifts relative to tetramethylsilane are reported on the ppm scale. The molecular weights of the polymers were determined by size exclusion chromatography (SEC) in THF using a Viscotek SEC system, which consists of a Viscotek VE1122 HPLC pump coupled with a Viscotek TDA Triple detector and a Viscotek 2501 UV detector operated at 260 nm. A set of ViscoGEL columns (G3000H, G4000H and G5000H) was used and calibrated using a set of polystyrene standards in THF. Differential scanning calorimetric (DSC) measurements and thermogravimetric analyses (TGA) were performed on a TA Instrument DSC 2920 and on a TA Instrument TGA 2950, respectively, using a heating rate of 10 °C min^{-1}. Absorption spectra were collected on a UV-Vis-NIR spectrophotometer (Cary 5000, Varian) over a wavelength range from 300 to 2100 nm. A double beam mode was used with a pure solvent cuvette placed in the reference channel. The yield of the enrichment processes and the purity of the SWCNT materials obtained were evaluated from the absorption spectra based on the method described in the ESI.† Raman spectra were acquired with an InVia Raman microscope (Renishaw) from drop-cast samples, using 514 nm (2.41 eV), 633 nm (1.96 eV), and 785 nm (1.58 eV) laser excitation sources and 50× magnification objective lens. Spectra were recorded from 100–3000 cm^{-1}, with a resolution of 4 cm^{-1}. Photoluminescence excitation maps (PLE) were acquired using a custom-built system with a Ti-sapphire laser as the excitation source and InGaAs photodiode array for detection (extended sensitivity between 900 and 2100 nm). Spectra were obtained from solutions drawn into capillaries with a rectangular cross-section and 100 μm path lengths. Samples for transmission electron microscopy (TEM) studies were prepared by placing 1 drop of the enriched nanotube dispersions (~1 μg ml^{-1}) on the carbon film coated copper grid with the excess solution removed by touching with a piece of filter paper at the edge of the grid. TEM images were obtained with a Philips CM20 (LaB6 filament) electron microscope, operating at 120 kV. Scanning electron microscope (SEM) images were obtained using Hitachi s-4700 operated at 1 kV (charge contrast imaging mode on SiO_2/Si substrate). SEM images were taken from the channel of the TFT devices.

SWCNT enrichment by polymer extraction

A typical enrichment was conducted by dispersing 25 mg of SWCNTs into 50 ml of toluene with 20 mg of PFDD. The mixture was homogenized for 30 min at 30 °C using horn sonication (Branson Sonifier 250, maximum power, 200 W) with a 10 mm tip operated at a duty cycle of 40% and output of 40%. The dispersion was then centrifuged at a relative centrifuge force (RCF) of 7600*g* (8000 rpm on an SS-34 rotor) for 30 min. The supernatant was filtered through a Teflon membrane with 0.2 μm pore size to collect the extracted SWCNTs. The collected SWCNTs were rinsed twice with 5 ml of toluene to remove unbound PFDD, and then re-dispersed in 5 ml of toluene using bath sonication for 5–10 min. In order to recover more SWCNT material, multiple extractions were employed by repeating the above process on the residual material from the previous centrifugation.

TFT device test

TFT devices were fabricated on a silicon wafer with a 100 nm thick thermal oxide layer. The chip was first cleaned using Piranha solution (1 : 2 (v/v) of 98% H_2SO_4 and 35% H_2O_2) for 30 min at 80 °C. After thoroughly rinsing with distilled water and isopropanol, the chip was blow dried with nitrogen, and then 2 drops of the SWCNT solution (SWCNT concentration, 26 μg ml^{-1}; weight ratio of PFDD/SWCNTs, 5.4/1) were spread on the surface, and allowed to sit for 10 min under the solvent vapor. The excess solution was drained by slowly tilting the chip and the surface was rinsed with 5 ml of toluene. The coated chip was annealed at 200 °C for 1 h before the top contacts (5 nm Ti followed by 100 nm Pd) were deposited through a shadow mask using an e-beam evaporator. The active channel width was

100 μm and the channel length was 25 μm. I–V curves were collected on a probe station and the mobility was calculated from the I_{sd}–V_G transfer curve in the linear regime based on a parallel plate model (assumes full coverage and uses the oxide capacitance).[57]

Results and discussion

Polymer preparation

Alkyl groups with a length from C10 to C18 have been introduced to the 9 position of the fluorene monomer to obtain a series of PFs. Scheme 1 depicts the synthetic route for polymer preparation. The alkylation of 2,7-dibromofluorene could be done in DMSO in the presence of a strong base, NaOH or KOH. KOH powder was preferred when making the octadecyl (C18) derivative. The products were purified by re-crystallization in acetone except for C10. This product is a liquid and was purified by column chromatography using hexanes as the eluent. The polymerization was effected by the Suzuki coupling reaction catalyzed by $(PPh_3)_4Pd(0)$ (see ESI for further details†) and the basic characterization data are listed in Table 1.

Factors that affect the enrichment

Molecular weight. Inspired by a very encouraging result in preliminary tests which showed that PFDD with a molecular weight (Mn) of 21.7 kDa could disperse SWCNTs effectively and yield a high sc-purity in the extraction, we undertook sc-SWCNT extractions using a series of PFDDs with different molecular weights. We observed that PFDD with a molecular weight lower than 8000 Da had a poor capability to disperse the SWCNTs. This result is consistent with the observation that PFDD-type oligomers with at least 8 repeating units are required for a good dispersion of small-diameter SWCNTs.[69] With molecular weights above 10 000 Da, there is no apparent difference in the capability to disperse and to selectively extract sc-SWCNTs. However, PFDDs with molecular weights (Mn) larger than 45.0 kDa significantly increased the viscosity of the polymer stabilized nanotube solutions causing practical difficulties in handling the material during processing. An optimum PFDD molecular weight between 10 000 and 30 000 Da has been identified. This molecular weight can be achieved by simply adjusting the ratio of dibromide and bis(boronate) monomers in the polymerization feed. Table 1 lists the number average molecular weight (Mn) and polydispersity index (PDI) of the polymers used to enrich SWCNTs in this work.

Table 1 Characterization data for PFs. Decomposition temperature at 1% weight loss ($T_d^{1\%}$) and glass transition temperature (T_g) were measured from TGA and DSC curves which are displayed in Fig. S1.

Polymer	PFO	PFD	PFDD	PFTD	PFOD
Mn (kDa)	26.7	13.6	21.7	13.4	23.7
PDI	2.4	2.7	4.1	3.0	4.2
T_g (°C)	136	101	48	40	35
$T_d^{1\%}$(°C)	390	380	381	374	382

Polymer side chain length. Though 9,9-dialkylfluorene homopolymers with short alkyl chains, including octyl, hexyl, and 2-ethylhexyl, can be used to enrich sc-SWCNTs with small diameters such as HiPco and CoMoCat nanotubes, these homopolymers were not able to effectively disperse large-diameter SWCNTs.[67] It was reported that the dispersing capability of PFO dramatically drops off when the diameter of nanotubes is above ~1.1 nm.[67] In this study, a series of 9,9-di-*n*-alkylfluorene homopolymers with alkyl groups varying from C8 to C18 were tested to extract sc-SWCNT at a SWCNT concentration of 0.5 mg mL^{-1} and a polymer/SWCNT ratio of 0.8 in toluene. A comparative test showed that PFO extracted only trace amounts of nanotubes in toluene. In contrast, polymers

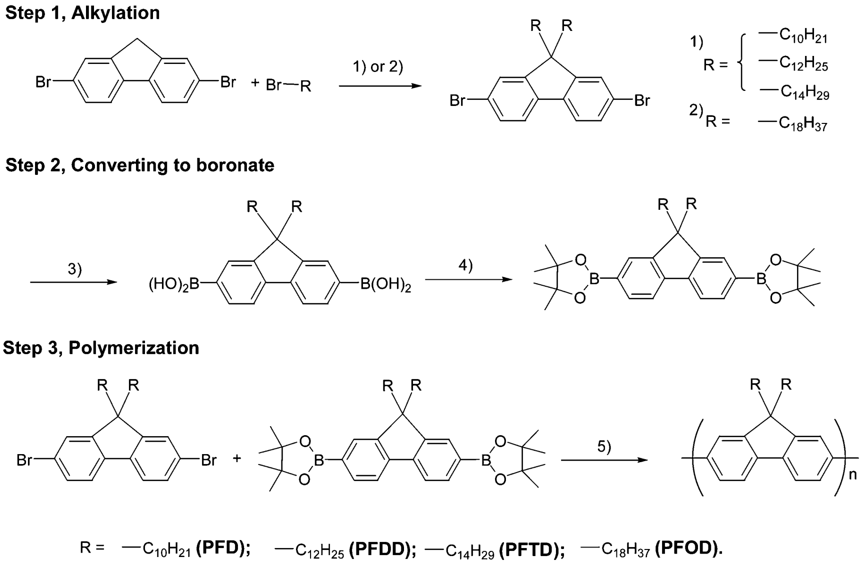

Scheme 1 Synthetic route for the preparation of poly(9,9-dialkylfluorene)s. (1) 50% NaOH and $C_6H_5CH_2N(C_2H_5)_3Cl$ in DMSO at 60 °C for 16 h; (2) KOH (powder), KI in DMSO at 50 °C for 3 h; (3) 2.1 eq. *n*-BuLi in THF at −78 °C for 1 h, followed by adding 4.0 eq. $B(OiPr)_3$, at −78 °C and then at RT for 10 h; (4) 3 eq. pinacol in toluene at reflux for 3 h. (5) 1 mol% $(PPh_3)_4Pd(0)$, Aliquat 336 in 2M Na_2CO_3 and toluene at reflux for 20 h.

with *n*-alkyl groups having 10, 12, 14, and 18 carbons were highly effective at dispersing and extracting sc-SWCNTs to yield a high purity of the extracted materials as judged by their absorption spectra (Fig. S7 in ESI†). This figure shows that the nanotubes enriched by PFD, PFDD, PFTD and PFOD have similar absorption spectra with the yields of sc-SWCNTs (η) being 5.3%, 6.8%, 5.4% and 6.4%, respectively, and the absorption peak ratios (ϕ_i) being 0.416, 0.403, 0.410 and 0.404, respectively. However, the UV signal of the solution resulting form the PFO extraction is very weak due to the very low concentration and thus the spectrum is not shown in Fig. S7.† Here the yield is defined as the mass percentage of the enriched sc-SWCNTs relative to the total mass of SWCNTs present in the starting material, and was calculated from the absorption spectra as described in the ESI.† The absorption peak ratio (ϕ_i) is defined as the ratio of the integrated area of the M11 and S22 peak envelop over the total area in this region. Details about ϕ_i, which correlates with the sc-SWCNT content in the sample, are described in the ESI (Fig. S6†). A high ϕ_i value reflects a high sc-purity, with the highest value being 0.416 (see Fig. S7 in the SI†). These results indicate the high effectiveness of enrichment with the ϕ_i values increasing from 0.082 for the raw sample to above 0.40 for the enriched materials, where the metallic (M11) peaks are no longer visible in the absorption spectra. We conclude that fluorene homopolymers with alkyl side chains longer than 10 carbons are effective at dispersing large-diameter SWCNTs and provide a high selectivity for the enrichment of sc-nanotubes. Though these four polymers gave very similar yields and sc-purity for the enrichment, polymers with longer side chains have a higher potential to solubilize the nanotubes, thus providing SWCNT dispersion with greater colloidal stability and fewer bundles. However, nanotube dispersions with longer alkyl side-chain polymers possess higher viscosities, making the filtration step problematic. All of these effects led us to select the PF with C12 side chains (PFDD) for detailed enrichment studies.

PFDD/SWCNT ratio. A series of PFDD/SWCNT ratios from 0.25 to 8.0 were evaluated for nanotube enrichment. Fig. 1 shows that a ratio of 0.5 gives the deepest valley of the absorption curve around 640 nm, indicating the highest sc-purity. The ϕ_i value of this enriched sample reached 0.403. This value is slightly higher than that recently reported by Blackburn for a sample of SWCNTs that was believed to have >99% sc-content,[67] (see Fig. S5 in ESI for details†). Hence we believe this sample with ϕ_i value over 0.40 also has a sc-purity higher than 99%. As the PFDD/SWCNT ratio increases, the purity progressively decreases with metallic peaks eventually appearing at 646 and 696 nm and the absorption background in the valley at 640 nm becoming gradually stronger. It is interesting that the extraction at the lowest ratio (0.25) did not give the highest purity. Its ϕ_i value is only 0.363, lower than the value (0.403) at the ratio of 0.5. This phenomenon may be related to the extremely low yield for this extraction (0.7%). At this polymer/SWCNT ratio, only very small amounts of solid were extracted from the dispersion which may include non-tube impurities such as fullerene derivatives and small carbon particle that were present in the raw SWCNT sample. They have high solubilities in toluene and are easily dispersed into the solution during the polymer extraction.

The sc-purity of this series of samples was also investigated by Raman scattering, see Fig. 1B. The RBM (radical breath mode) of the spectra excited at 785 nm shows that the 0.5 sample has a nearly flat baseline in the metallic region from 135 to 175 cm^{-1}, confirming a high sc-purity. As the PFDD/SWCNT ratio was increased from 0.5 to 8.0, a broad metallic band centered at 162 cm^{-1} gradually appeared, with an intensity almost linearly correlated with ϕ_i, see the inset of Fig. 1B. This shows that ϕ_i is indeed a useful metric for a quick evaluation of the relative purity of sc-SWCNT samples.

The results tabulated in Fig. 1A show that the extraction yield increased significantly at higher polymer/SWCNT ratios. At a ratio of 0.25, almost no nanotubes were extracted. As the ratio was increased from 0.25 to 0.5, the yield increased from 0.7% to 4.5%, and as the ratio was further increased to 8.0, the yield reached 20.4%. It would appear that increasing the amount of polymer in the extraction increases yield but with some sacrifice

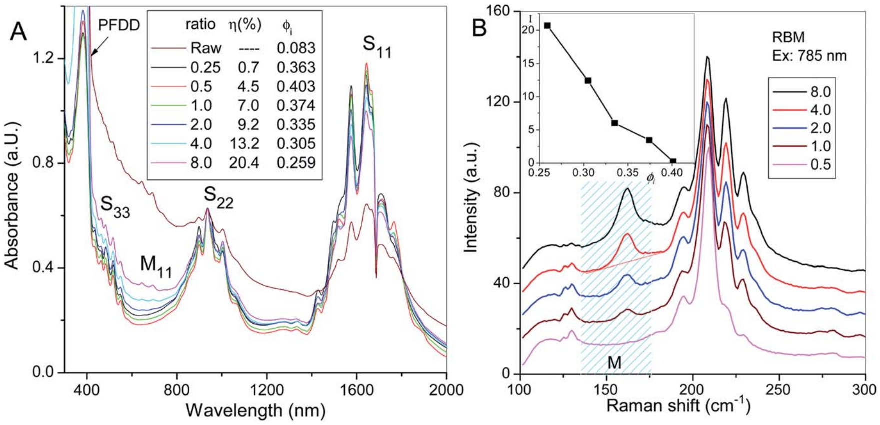

Fig. 1 Absorption spectra (A) and Raman spectra (B) in the RBM region excited at 785 nm for the samples extracted by PFDD at a tube concentration of 0.4 mg mL^{-1} and polymer/SWCNTs ratios of 0.25, 0.5, 1.0, 2.0, 4.0, and 8.0, in toluene. The relative intensity of the metallic band at 162 cm^{-1} (normalized to the sc-band at 209 cm^{-1}) was also plotted against the ϕ_i value of the sample as the inset in (B).

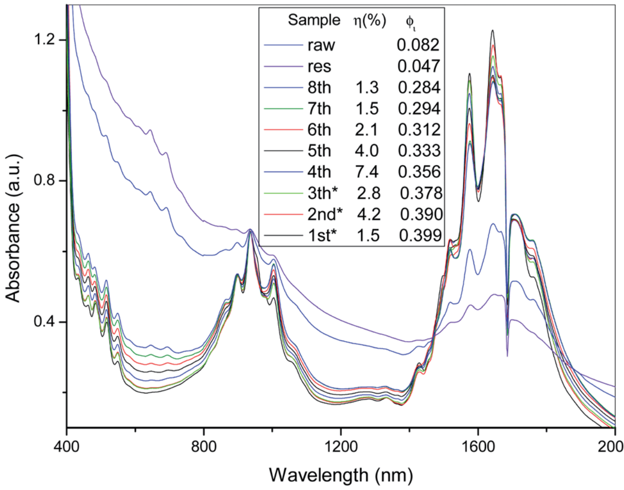

Fig. 2 Absorption spectra, yield (η) and ϕ_i ratio of the enriched sc-SWCNTs for each extraction from the multi-extraction process. The spectra were normalized to the peak at 936 nm. The SWCNT concentration was 1.0 mg mL^{-1} and the polymer/SWCNT ratio was 0.8 for the first three extractions (marked by *) and 0.33 mg mL^{-1} and 0.4, for the succeeding five extractions. Spectra of the dispersion before the 1st centrifugation (raw), and the residual of the 8th extraction (res) dispersed in 0.5 mg mL^{-1} PFDD solution have also been plotted for comparison.

of sc-purity. Ratios between 0.5 and 1.0 give high purities and reasonable yields of 5–10% after only a single extraction.

Multiple extractions. Though the extraction at a low polymer/SWCNT ratio of 0.5–1.0 provided a high sc-purity, the yield was relatively low (5–10%). Since the raw sample contains ~53% SWCNTs and approximately 70% of these are semiconducting, it is obvious that a single extraction only recovers a small portion of the sc-nanotubes present in the source material. Therefore, a multiple extraction process was explored. Compared in Fig. 2 are the absorption spectra that result from 8 successive extractions. The spectra of the dispersion of the raw material (raw), and the residual of the 8th extraction (res) are also displayed for comparison. The calculated yield and ϕ_i ratio for each extraction are tabulated in the figure. Note that the first three extractions were done at a SWCNT concentration of 1.0 mg mL^{-1} and a polymer/SWCNT ratio of 0.8, and the succeeding five extractions were conducted using a SWCNT concentration of 0.33 mg mL^{-1} and a polymer/SWCNT ratio of 0.4. This adjustment was found to be necessary to maximize yield by compensating for the reduced sc-SWCNT content in the extraction residual, which was used as the starting material for subsequent extractions.

Fig. 2 shows that the products from the first three extractions had a high sc-purity with M11 peaks completely eliminated with ϕ_i ratios of 0.378–0.399. However, as the number of extractions increased two metallic peaks at 646 and 696 nm gradually appeared and the ϕ_i ratio was reduced from 0.399 for the first extraction to 0.284 for the last extraction, indicating a gradual decrease of the sc-purity. Based on the method used by NanoIntegris as described in the SI, the first 3 extractions provided a sc-purity estimate >99%, while as the last 5 extractions provide a purity estimate of 98–99%. It should be noted that the quoted sc-purities are not absolute purities. The yield from the first three extractions were relatively low, adding up to only 8.5%, but the yield from the fourth extraction was much higher, jumping to 7.4%, due to the use of a larger quantity of solvent (3 fold). The yield for the last three extractions dropped significantly, indicating that only a very small amount of sc-nanotubes are still accessible in the residual solid. The combined yield from all 8 extractions was 25%, much smaller than the estimated sc-SWCNT ratio in the raw material (70%). This can be partly attributed to the affinity of the polymer extraction for the near armchair nanotubes. The photoluminescence excitation (PLE) mapping study shown below indicates that near-armchair species (10,9) dominate the enriched material. Another reason might be the presence of SWCNT bundles in the raw material. SWCNTs in very tight bundles would be almost inaccessible to polymer extraction. It should be noted that aggressive horn sonication was only used for the dispersion of the raw material for the first extraction, while mild bath sonication was used in subsequent extractions to help preserve the average length of the SWCNTs above 1 micron (*vide infra*). The low sonication power used might not be strong enough to dissociate the tightest bundles. This assumption was verified by comparing the absorption spectrum of the residual after the last extraction (res) with that of the raw material (raw) in Fig. 2. This comparison shows that while the residual has a significantly reduced intensity of S11 and S22 peaks compared to the M11 peak (indicating a large fraction of the accessible sc-tubes were separated by the multiple extractions), significant amounts of sc-SWCNTs still remain in the residual.

Enrichment mechanism. The enrichment simply entails dispersing SWCNTs in a PFDD/toluene solution using horn sonication, followed by a centrifugation of the dispersed mixture. During this process, SWCNTs are exfoliated from bundles and aggregates, and become wrapped by the polymer to form stabilized dispersions in toluene. The less stable dispersed tubes will re-form bundles or aggregates. The non-dispersed materials and the re-formed aggregates are removed by centrifugation. Therefore, the enrichment relies on the tightness of bundles and the SWCNT capability to re-aggregate in the dispersion.

In order to evaluate both factors, tightness of the bundles and capability to re-aggregate, the enrichment process can be divided into two steps: the first is a coarse enrichment in which dispersible materials can be separated from non-dispersible material and the second step is a fine enrichment involving the removal of reformed aggregates of the less stable nanotubes from the stably dispersed sc-SWCNTs. Hence a two-step time lapsed study was designed. First, the raw PFDD/SWCNT mixture at 0.8 mg mL^{-1} SWCNT concentration and 1.0/1.0 PFDD/SWCNT ratio was horn sonicated for 30 min at 30 °C and was immediately centrifuged at 12 500 rpm (RCF 18 700*g*) for 5 min to remove non-dispersed solid. Then the supernatant of this centrifugation was divided into several samples, which were allowed to stand for different lengths of time prior to another 5 min centrifugation to remove re-aggregated material that had formed while standing. This experiment allows us to assess

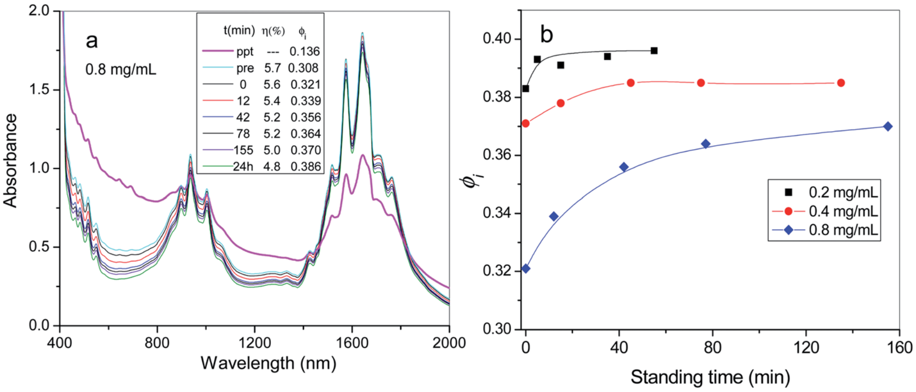

Fig. 3 (a) UV spectra of the supernatant from the 1st centrifugation (pre) and the 2nd centrifugation after the supernatant of the 1st centrifugation were allowed to stand for 0, 12, 42, 78, 155 min. The UV spectra of the supernatant (24 h) and precipitate (ppt) of the 2nd centrifugation (for 1 h) after 24 h standing is also plotted for comparison. The yield (η) and ϕ_i values for each sample are also listed. (b) The variation of ϕ_i values with standing time. The SWCNT concentration of the raw dispersion is 0.2, 0.4, 0.8 mg mL^{-1}, and their PFDD/SWCNT ratio is 1.0/1.0.

whether the sc-tubes in the initial dispersion were selectively exfoliated from the raw SWCNTs during sonication and whether the m-tubes in the dispersion re-aggregate more rapidly than sc-tubes upon standing, thus leading to high purity sc-SWCNTs.

The supernatants of the 1st centrifugation and the 2nd centrifugation of the each sample with different standing time were examined by UV spectroscopy with the absorption spectra displayed in Fig. 3a. It shows the supernatant from the 1st centrifugation (pre) possesses a much higher sc-purity than the raw material (see Fig. 2) with the ϕ_i value increased from 0.083 to 0.306, corresponding to the sc-/m- ratio increased from 70/30 to about 95/5. Note this sample is centrifuged for 5 min right after sonication, and thus re-aggregation of dispersed tubes during this short centrifugation time is negligible at this concentration. This suggests that the sc-enrichment observed at this stage results from preferential exfoliation of sc-tubes. This result might suggest m-tubes provided a stronger inter-tube interaction in bundles.

Fig. 3a also compares the UV spectra of the supernatants from the 2nd centrifugations. A sample that had been left to stand for 24 h and then centrifuged for 1 h represents the maximum aggregated sample (24 h). The precipitate from this sample was re-dispersed and its UV spectrum is also included (ppt). The inset in Fig. 3a shows that the sc-purity of the supernatant increases with standing time, with the ϕ_i value improving from 0.321 at 0 min to 0.370 at 155 min. The latter value compares well with the 24 h sample for which the ϕ_i value was 0.386. This shows that the m-tubes also preferentially aggregated in the supernatant, which necessarily leads to further sc-enrichment. As the standing time was increased, the enriched sc-tubes were obtained in slightly lower yields (approx 5%) but with consistently higher purity (see inset in Fig. 3a). These results indicate that the standing time is an important factor to influence both the yield and sc-purity of the enriched sc-SWCNTs. Furthermore, the residual (ppt) of the 24 h sample exhibits a very low sc-purity, with a ϕ_i value of 0.136, which is much lower than that of supernatant (0.386), and only slightly higher than the raw material (0.083). This once again confirms that the selective removal of m-tubes by the 2nd centrifugation is due to the faster aggregation of the m-tubes. Indeed, with the appropriate time delay, 5 min centrifugation at 12 500 rpm (RCF 18 700*g*) is sufficient to remove most of the metallic SWCNTs.

The same experiments for two other SWCNT concentrations (0.4 and 0.2 mg mL^{-1}) were also conducted. The variation of ϕ_i as a function of standing time is compared in Fig. 3b for all three SWCNT concentrations (0.8, 0.4 and 0.2 mg mL^{-1} with PFDD/SWCNT ratio = 1.0/1.0). This plot shows that ϕ_i levels off after 40 min at 0.4 mg ml^{-1} but after only 10 min at 0.2 mg mL^{-1}. Thus, aggregation occurs more rapidly at lower SWCNT concentrations. Therefore, the centrifugation protocol can be adjusted to account for the re-bundling that occurs during centrifugation. As can be seen in Fig. 3b, the ϕ_i value plateaus at 10, 40 and 80 min for 0.2, 0.4 and 0.8 mg mL^{-1} SWCNT concentrations, respectively. From a processing stand point a dispersion can either stand for a longer time followed by a short time centrifugation, or be centrifuged immediately after dispersion for a longer time (*e.g.* 30 min) to obtain material of similar sc-purity. It is also clear from Fig. 3b that decreasing concentrations lead to higher sc-purities, as evidenced by higher ϕ_i values.

Detailed characterization of the enriched sc-SWCNTs and TFT device evaluation

The optimized enrichment procedure. From the above discussion, we know that extraction conditions with a SWCNT concentration of 0.4 to 1.0 mg mL^{-1} and a polymer/SCWNT ratio of 0.5 and 1.0 will give a high purity and a reasonable yield. Therefore, an optimized enrichment protocol was selected within this operating window, where the raw SWCNT material was mixed with PFDD in toluene at a PFDD/SWCNT weight ratio of 0.8 and a SWCNT concentration of 0.5 mg mL^{-1}. The mixture was homogenized by horn sonication for 30 min at 30 °C to promote polymer wrapping. The homogenized dispersion was centrifuged at a RCF of 7600*g* for 30 min, the supernatant was filtered to collect a dark-yellow solid, which was rinsed with toluene to remove unbound polymer. This enriched sample was

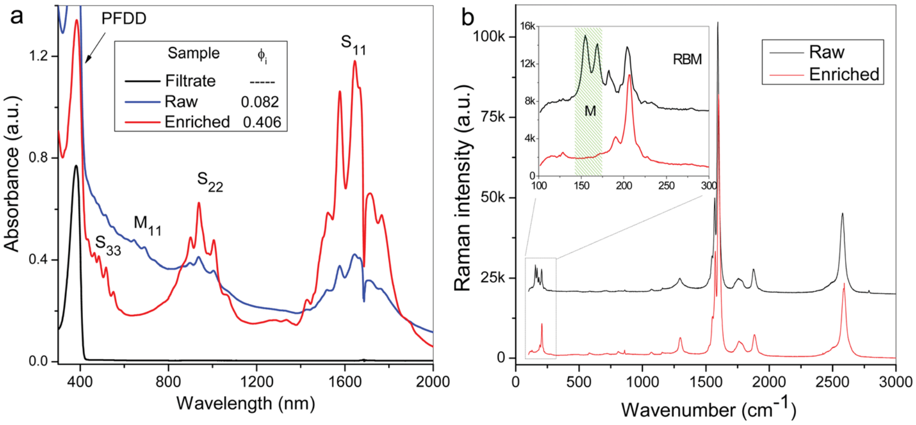

Fig. 4 Absorption (a) and Raman (excited at 785 nm) (b) spectra of the raw SWCNT dispersion and the enriched sc-SWCNTs re-dispersed in toluene. The absorption spectra of the filtrate from this process is included for comparison. The solutions of the raw dispersion and the filtrate were diluted 20x for this measurement.

re-dispersed in toluene by bath sonication for 5–10 min, and its absorption spectrum was measured, see Fig. 4a (Enriched). For comparison, the absorption spectra of the filtrate and the homogenized raw dispersion before the centrifugation (Raw) were also measured, where these two solutions were diluted by a factor of 20 (Fig. 4). No SWCNT signal can be seen in the spectrum of the filtrate, indicating that the filtration through a 0.2 μm Teflon membrane collected all dispersed nanotubes. This result is consistent with the length of the SWCNTs having been largely preserved. Note that the intensity of the PFDD absorption band at 380 nm of the filtrate is only about 63% of that of the raw SWCNT dispersion, which means that a large amount of PFDD is wrapped on the SWCNTs in the dispersion. Well-resolved S_{11}, S_{22} and S_{33} peaks can be seen for the enriched sample. It can also be seen that the M_{11} peaks at 640 and 690 nm in the raw sample have been completely removed in the enriched sample and that the valleys at approximately 640 nm and 1200 nm have become much deeper after the separation with the ϕ_i ratio increasing from 0.082 for the raw material to 0.406 for the enriched sample, thus demonstrating that a high sc-purity can be realized in a single extraction.

These enriched and raw samples were also characterized by Raman scattering with the spectra compared in Fig. 4b. The spectra were collected from thin film samples using 785 nm excitation wavelength. They were prepared by casting the dispersions onto glass slides. Fig. 4b shows that the metallic peaks in the RBM region are completely eliminated after the enrichment, consistent with the UV-vis-NIR absorption spectrum.

PLE mapping. A photoluminescence excitation (PLE) map for the PFDD enriched sc-SWCNT sample is presented in Fig. 5. Well resolved (S_{22}, S_{11}) maxima can be seen, indicative of properly individualized (*i.e.*, separated) nanotubes. Up to 19 (n, m) species contribute to the spectrum, with 8 or 9 having peak intensities higher than or close to 0.5 (see Fig. S8 in ESI for assignments†). Among these, one peak is stronger and can be assigned to the near-armchair (10,9) SWCNTs with S_{11} = 1570 nm and S_{22} = 910 nm. Based on relative intensity alone, we conclude that twice as much (10,9) nanotubes were present as other chiralities. This selectivity of polyfluorenes towards near-armchair chiralities is consistent with an earlier report by Nicholas.[22] Furthermore, the eight other major chiralities have a diameter from 1.25–1.35 nm, and all 19 chiralities identified in Fig. 5 showed the diameter in a range of 1.20 and 1.40 nm, (blue and cyan area in Fig. S8,† respectively), indicating a narrow diameter distribution of this enriched sample. Happily, the integration curves of the PL emission slices of the PLE mapping showed a one to one correspondence with the S_{11} absorption peaks (as shown in Fig. S9 in ESI†), indicating the absorption and emission signals are dominated by individualized nanotubes.

SWCNT film morphology and thin film transistor device performance. Besides high sc-purity, the enriched sc-SWCNTs must also possess adequate length and crystallinity so as to

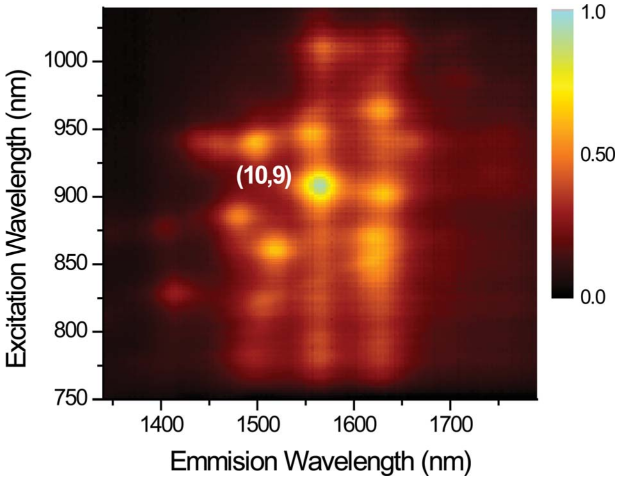

Fig. 5 The photoluminescence excitation map of the sc-SWCNTs enriched by PFDD in toluene. A maximum of 8 or 9 chiralities appear to dominate the spectrum with the (10,9) species being most abundant (emission at 1570 nm, excitation at 910 nm).

form uniformly dense networks in the transistor channel and thus provide optimum device performance. One attribute of the laser derived material is the considerable length of the pristine SWCNTs.[17] Tube length is particularly important when scaling devices with printing resolution limits in mind, which require minimum inter-tube contact resistance while printing relatively large channel devices using current printing technology. In the enrichment process, the nanotubes will often be broken by the high power sonication used to disperse and de-bundle nanotubes. The length of the enriched nanotubes was therefore evaluated by TEM and SEM with the images displayed in Fig. S10 (see ESI†). The TEM image shows straight individual nanotubes with few bundles. A number average length of 1.3 μm (length average, 1.8 μm) was estimated based on a sampling of ~200 nanotubes in the SEM image. This result was also confirmed by AFM analysis, where an average tube length of 1.4 μm was determined.

In order to find proper coating conditions to generate a nanotube network with suitable density for device fabrication, different concentrations and coating methods were evaluated, and the morphology of the deposited network was verified by SEM. It was found that uniform and high density nanotube networks could be formed using a simple drop-casting method (Fig. 6B). This was accomplished by spreading two drops of the SWCNT solution (26 μg ml^{-1}) on freshly cleaned SiO_2/Si surfaces under toluene vapor for 10 min, after which the excess solution was drained and the surface was rinsed with 5 ml of toluene. Importantly, this nanotube network was directly coated on a bare SiO_2/Si substrate without any surface coating. Previously, it has been common to use an intermediate adhesion layer (such as poly-L-lysine) to assist in the creation of a nanotube network.[27,32] The dense SWCNT network we have obtained in such a simple manner is comparable to the high density nanotube networks prepared by more laborious methods such as chemical self-assembly.[70] Furthermore, our enriched sc-SWCNTs have allowed the use of a simple drop-cast process for device fabrication that is compatible with many existing printing techniques.

The top contact, bottom gate TFT device with 25 μm channel length and 100 μm channel width is schematically shown in Fig. 6A. It was prepared by depositing the source/drain electrodes on the sc-SWCNT network *via* evaporation through a shadow mask. Typical transfer and output curves are also shown in Fig. 6, from which a mobility of 32 $\mathrm{cm}^2\ \mathrm{V}^{-1}\ \mathrm{s}^{-1}$ with on/off ratio of 1.7×10^6 was calculated. From the output curve in Fig. 6D, the sheet resistance of the device is 170 kΩ square^{-1} when the gate voltage is −5 V. All twenty-five devices prepared on a chip were evaluated and provided good transistor

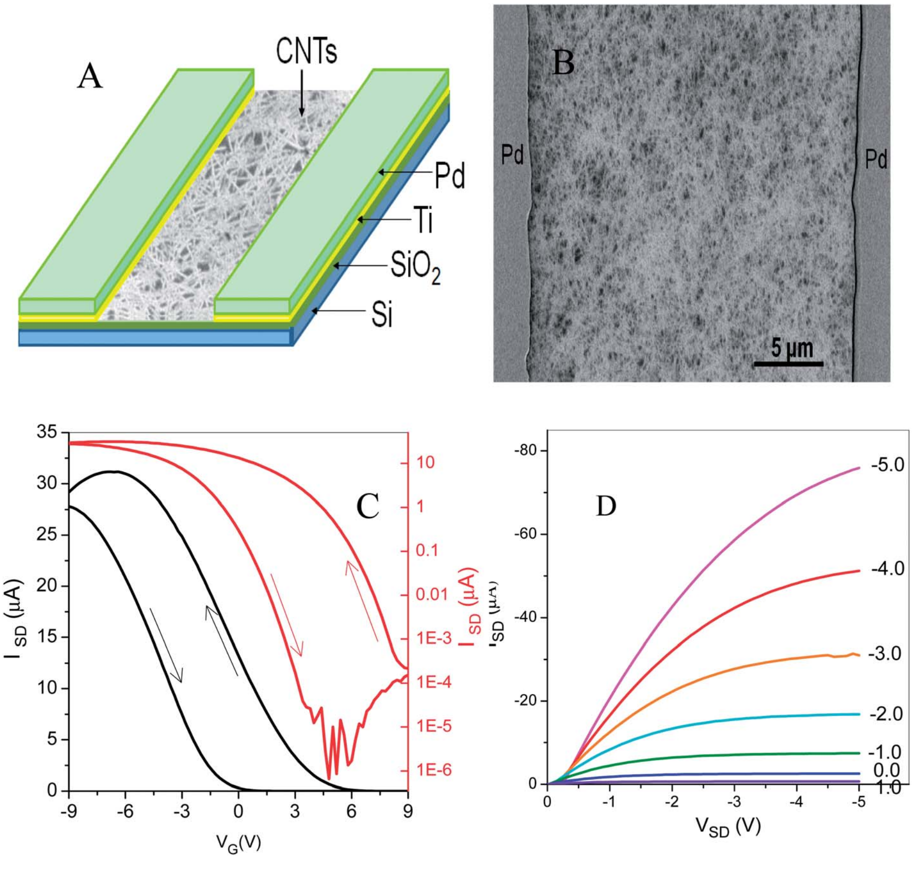

Fig. 6 Device configuration (A), SEM image (B), transfer curve (C) and output curves (D) of a typical TFT device with a channel length of 25 μm and a width of 100 μm (top contact source/drain electrodes with 5 nm Ti/100 nm Pd). The transfer curve was taken at a source-drain voltage of 1.0 V. The device was made by drop-casting a PFDD enriched sc-SWCNT solution (0.026 mg mL^{-1}) on a freshly cleaned SiO_2/Si substrate.

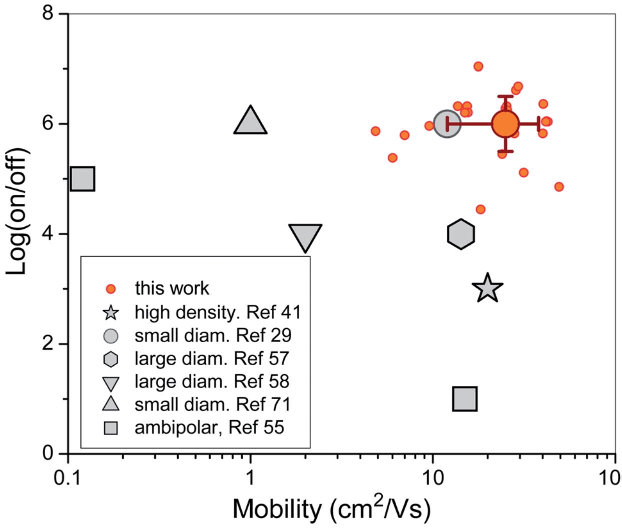

Fig. 7 The performance of all 25 TFT devices prepared on a SiO_2/Si chip with PFDD enriched sc-SWCNTs. The data was collected as described in Fig. 6. Recently reported performance data for conjugated polymer enriched sc-SWCNTs with small and large diameter SWCNTs are also plotted for comparison.

performance with an average mobility of 26 ± 14 $cm^2\ V^{-1}\ s^{-1}$ and on/off ratio in a range of 10^4 to 10^7 (see Fig. 7). The mobility of the 25 devices varied from 5 to 43 $cm^2\ V^{-1}\ s^{-1}$. SEM images in Fig. S11† of ESI showed a highly uniform nanotube network formed in all of the 25 devices on the chip with a nanotube density of ~64 tubes per μm^2. This result indicates that the mobility variation of the devices is not only attributed to the network density, but also another type of spatial non-uniformity such as a surface contaminant either directly on the substrate, at nanotube–nanotube junctions or at the nanotube-source/drain interface. In general, this data-set demonstrates improved performance when compared to the best results reported thus far for conjugated polymer enriched sc-SWCNTs (Fig. 7).[29,41,55,57,58,71] In particular, a device with a denser SWCNT network prepared using the same procedure but without solvent rinsing provided a TFT mobility of 58 $cm^2\ V^{-1}\ s^{-1}$ and on/off ratio of 1 × 10^4, confirming the high purity of our enriched sc-SWCNTs.[72] The devices were prepared using a simple drop-casting method on clean Si/SiO_2 substrates without any need for an adhesive surface treatment. It should also be noted that the PFDD, with ~80% weight ratio in the dispersion, has no apparent detrimental effect on device performance, as evidenced by the excellent performance of a device formed by the drop-cast sc-SWCNT network which was not rinsed.

Conclusions

In summary, we have demonstrated the exceptional selectivity of PFs with alkyl side-chains containing ≥10 carbons in the dispersion and extraction of large-diameter, laser-derived sc-SWCNTs. Polymers with molecular weights over 10 000 Da were required to effectively disperse the nanotubes and to obtain enrichment. The yield and sc-purity of the enriched fraction are affected by the nanotube concentration and polymer/SWCNT ratio. A sc-purity higher than 99% (as assessed by UV-vis-NIR spectroscopy) with a yield of 5–10% was easily obtained from a single extraction at a SWCNT concentration of 0.4–1.0 mg mL^{-1} and a polymer/SWCNT ratio of 0.5–1.0. Increasing this ratio to 8.0 increases the yield to ~20%, but with a somewhat reduced sc-purity. A multiple extraction process was developed to push the yield up to 25% while maintaining a high sc-purity. TFT devices using enriched sc-SWCNTs as the channel material provided an average current on/off ratio of 1.8 × 10^6 and an average mobility of 27 $cm^2\ V^{-1}\ s^{-1}$ for all 25 devices with a 25 μm channel length prepared on a single chip.

Notes

The authors declare no competing financial interest.

Acknowledgements

The authors would like to thank Joseph McKee and Hue Tran for their work on the TFT device fabrication, Jeff Fraser for SEM study and Xiaomei Du for TEM investigation. We would also like to thank Jens Kroeger and Nathan Yoder from Raymor Industries Inc for valuable discussions and for supplying their plasma derived SWCNT products.

References

1 S. Iijima, *Nature*, 1991, **354**, 56–58.
2 S. Iijima and T. Ichihashi, *Nature*, 1993, **363**, 603–605.
3 R. Saito, G. Dresselhaus and M. S. Dresselhaus, *Physical Properties of Carbon Nanotubes*, Imperial College Press, 1998.
4 S. Cataldo, P. Salice, E. Menna and B. Pignataro, *Energy Environ. Sci.*, 2012, **5**, 5919–5940.
5 S. Berson, R. de Bettignies, S. Bailly, S. Guillerez and B. Jousselme, *Adv. Funct. Mater.*, 2007, **17**, 3363–3370.
6 J. M. Holt, A. J. Ferguson, N. Kopidakis, B. A. Larsen, J. Bult, G. Rumbles and J. L. Blackburn, *Nano Lett.*, 2010, **10**, 4627–4633.
7 E. Adam, C. M. Aguirre, L. Marty, B. C. St-Antoine, F. Meunier, P. Desjardins, D. Ménard and R. Martel, *Nano Lett.*, 2008, **8**, 2351–2355.
8 Q. Cao, H. S. Kim, N. Pimparkar, J. P. Kulkarni, C. Wang, M. Shim, K. Roy, M. A. Alam and J. A. Rogers, *Nature*, 2008, **454**, 495–500.
9 G. Gruner, *J. Mater. Chem.*, 2006, **16**, 3533–3539.
10 H. Gu and T. M. Swager, *Adv. Mater.*, 2008, **20**, 4433–4437.
11 M. E. Roberts and S. C. B. Mannsfeld, *Org. Electron.*, 2009, **10**, 377–383.
12 A. Star, T. R. Han, V. Joshi, J. C. P. Gabriel and G. Gruner, *Adv. Mater.*, 2004, **16**, 2049–2052.
13 S. Peng, K. Cho, P. Qi and H. Dai, *Chem. Phys. Lett.*, 2004, **387**, 271–276.
14 E. S. Snow, F. K. Perkins, E. J. Houser, S. C. Badescu and T. L. Reinecke, *Science*, 2005, **307**, 1942–1945.
15 M. E. Roberts, M. C. LeMieux and Z. Bao, *ACS Nano*, 2009, **3**, 3287–3293.

16 R. Saito, M. Fujita, G. Dresselhaus and M. S. Dresselhaus, *Appl. Phys. Lett.*, 1992, **60**, 2204–2206.

17 C. T. Kingston and B. Simard, *J. Nanosci. Nanotechnol.*, 2006, **6**, 1225–1232.

18 K. S. Kim, G. Cota-Sanchez, C. T. Kingston, M. Imris, B. Simard and G. Soucy, *J. Phys. D: Appl. Phys.*, 2007, **40**, 2375–2387.

19 R. E. Sturgeon, J. W. Lam, A. Windust, P. Grinberg, R. Zeisler, R. Oflaz, R. L. Paul, B. E. Lang, J. A. Fagan, B. Simard and C. T. Kingston, *Anal. Bioanal. Chem.*, 2012, **402**, 429–438.

20 See http://www.raymor.com.

21 F. Hennrich, R. Krupke, S. Lebedkin, K. Arnold, R. Fischer, D. E. Resasco and M. M. Kappes, *J. Phys. Chem. B*, 2005, **109**, 10567–10573.

22 (*a*) A. Nish, J.-Y. Hwang, J. Doig and R. J. Nicholas, *Nat. Nanotechnol.*, 2007, **2**, 640–646; (*b*) W. Zhou, S. Zhan, L. Ding and J. Liu, *J. Am. Chem. Soc.*, 2012, **134**, 14019–14026; L. Ding, A. Tselev, J. Y. Wang, D. N. Yuan, H. B. Chu, T. P. McNicholas, Y. Li and J. Liu, *Nano Lett.*, 2009, **9**, 800–805; B. Yu, C. Liu, P. X. Hou, Y. Tian, S. S. Li, B. L. Liu, F. Li, E. I. Kauppinen and H. M. Cheng, *J. Am. Chem. Soc.*, 2011, **133**, 5232–5235.

23 A. Vijayaraghavan, F. Hennrich, N. Sturzl, M. Engel, M. Ganzhorn, M. Oron-Carl, C. W. Marquardt, S. Dehm, S. Lebedkin, M. M. Kappes and R. Krupke, *ACS Nano*, 2010, **4**, 2748–2754.

24 F. Hennrich, S. Lebedkin and M. M. Kappes, *Physica Status Solidi (B): Basic Research*, 2008, **245**, 1951–1953.

25 M. C. Hersam, *Nat. Nanotechnol.*, 2008, **3**, 387–394.

26 M. S. Arnold, A. A. Green, J. F. Hulvat, S. I. Stupp and M. C. Hersam, *Nat. Nanotechnol.*, 2006, **1**, 60–65.

27 V. K. Sangwan, R. P. Ortiz, J. M. P. Alaboson, J. D. Emery, M. J. Bedzyk, L. J. Lauhon, T. J. Marks and M. C. Hersam, *ACS Nano*, 2012, **6**, 7480–7488.

28 M. Zheng and E. D. Semke, *J. Am. Chem. Soc.*, 2007, **129**, 6084–6085.

29 X. Tu, S. Manohar, A. Jagota and M. Zheng, *Nature*, 2009, **460**, 250–253.

30 G. S. Tulevski, A. D. Franklin and A. Afzali, *ACS Nano*, 2013, **7**, 2971–2976.

31 R. Krupke, F. Hennrich, H. von Loehneysen and M. M. Kappes, *Science*, 2003, **301**, 344–347.

32 H. W. Lee, Y. Yoon, S. Park, J. H. Oh, S. Hong, L. S. Liyanage, H. Wang, S. Morishita, N. Patil, Y. J. Park, J. J. Park, A. Spakowitz, G. Galli, F. Gygi, P. H.-S. Wong, J. B.-H. Tok, J. M. Kim and Z. Bao, *Nat. Commun.*, 2011, **2**, 541.

33 Y. J. Park, J. M. Kim, H. W. Lee and Z. Bao, US 2012/0104328, and WO/2012/060601.

34 J. Y. Hwang, A. Nish, J. Doig, S. Douven, C. W. Chen, L. C. Chen and R. J. Nicholas, *J. Am. Chem. Soc.*, 2008, **130**, 3543–3553.

35 S. D. Stranks, A. M. R. Baker, J. A. Alexander-Webber, B. Dirks and R. J. Nicholas, *Small*, 2013, **9**, 2245–2249.

36 C. Y. Khripin, J. A. Fagan and M. Zheng, *J. Am. Chem. Soc.*, 2013, **135**, 6822–6825.

37 P. Avouris and R. Martel, *MRS Bull.*, 2010, **35**, 306–313.

38 M. Engel, J. P. Small, M. Steiner, M. Freitag, A. A. Green, M. C. Hersam and P. Avouris, *ACS Nano*, 2008, **2**, 2445–2452.

39 N. P. Guisinger and M. S. Arnold, *MRS Bull.*, 2010, **35**, 273–279.

40 F. Lemasson, J. Tittmann, F. Hennrich, N. Sturzl, S. Malik, M. M. Kappes and M. Mayor, *Chem. Commun.*, 2011, **47**, 7428–7430.

41 Q. Cao, S.-J. Han, G. S. Tulevski, Y. Zhu, D. D. Lu and W. Haensch, *Nat. Nanotechnol.*, 2013, **8**, 180–186.

42 P. R. L. Malenfant, W. V. Cicha, P. A. Bui and D. L. Simone, US20060045838A1, 2006; and US7247670, 2007.

43 P. R. L. Malenfant, J.-U. Lee, Y. Li and W. V. Cicha, US20060081882A1, and 2006; US7226818, 2007.

44 W. Yi, A. Malkovskiy, Q. Chu, A. P. Sokolov, M. L. Colon, M. Meador and Y. Pang, *J. Phys. Chem. B*, 2008, **112**, 12263–12269.

45 S. M. Keogh, T. G. Hedderman, E. Gregan, G. F. Farrell, G. Chambers and H. J. Byrne, *J. Phys. Chem. B*, 2004, **108**, 6233–6241.

46 S. M. Keogh, T. G. Hedderman, P. Lynch, G. F. Farrell and H. J. Byrne, *J. Phys. Chem. B*, 2006, **110**, 19369–19374.

47 J. Chen, H. Liu, W. A. Weimer, M. D. Halls, D. H. Waldeck and G. C. Walker, *J. Am. Chem. Soc.*, 2002, **124**, 9034–9035.

48 N. A. Rice, K. Soper, N. Zhou, E. Merschrod and Y. Zhao, *Chem. Commun.*, 2006, **47**, 4937–4939.

49 F. A. Lemasson, T. Strunk, P. Gerstel, F. Hennrich, S. Lebedkin, C. Barner-Kowollik, W. Wenzel, M. M. Kappes and M. Mayor, *J. Am. Chem. Soc.*, 2011, **133**, 652–655.

50 A. Stuparu, C. Stroh, F. Hennrich and M. M. Kappes, *Phys. Status Solidi B*, 2010, **247**, 2653–2655.

51 N. Sturzl, F. Hennrich, S. Lebedkin and M. M. Kappes, *J. Phys. Chem. C*, 2009, **113**, 14628–14632.

52 F. Chen, B. Wang, Y. Chen and L. J. Li, *Nano Lett.*, 2007, **7**, 3013–3017.

53 X. Zhou, J.-Y. Park, S. Huang, J. Liu and P. L. McEuen, *Phys. Rev. Lett.*, 2005, **95**, 146805.

54 S. Lebedkin, F. Hennrich, O. Kiowski and M. M. Kappes, *Phys. Rev. B: Condens. Matter Mater. Phys.*, 2008, **77**, 165429.

55 E. Gaufrès, N. Izard, L. Vivien, S. Kazaoui, D. Marris-Morini and E. Cassan, *Opt. Lett.*, 2009, **34**, 3845–3847.

56 S. Mouri, Y. Miyauchi and K. Matsuda, *J. Phys. Chem. C*, 2012, **116**, 10282–10286.

57 S. Z. Bisri, J. Ga, V. Derenskyi, W. Gomulya, I. Iezhokin, P. Gordiichuk, A. Herrmann and A. M. Loi, *Adv. Mater.*, 2012, **24**, 6147–6152.

58 F. Cheng, P. Imin, C. Maunders, G. Botton and A. Adronov, *Macromolecules*, 2008, **41**, 2304–2308.

59 W. Gomulya, G. D. Costanzo, E. J. F. de Carvalho, S. Z. Bisri, V. Derenskyi, M. Fritsch, N. Fröhlich, S. Allard, P. Gordiichuk, A. Herrmann, S. J. Marrink, M. C. dos Santos, U. Scherf and M. A. Loi, *Adv. Mater.*, 2013, **25**, 2948–2956.

60 H. Wang, J. Mei, P. Liu, K. Schmidt, G. Jiménez-Osés, S. Osuna, L. Fang, C. J. Tassone, A. P. Zoombelt, A. N. Sokolov, K. N. Houk, M. F. Toney and Z. Bao, *ACS Nano*, 2013, **7**, 2659–2668.

61 L. Qian, W. Xu, X. Fan, C. Wang, J. Zhang, J. Zhao and Z. Cui, *J. Phys. Chem. C*, 2013, **117**, 18243–18250.

62 M. Tange, T. Okazaki and S. Iijima, *J. Am. Chem. Soc.*, 2011, **133**, 11908–11911.

63 N. Berton, F. Lemasson, J. Tittmann, N. Sturzl, F. Hennrich, M. M. Kappes and M. Mayor, *Chem. Mater.*, 2011, **23**, 2237–2249.

64 F. Lemasson, N. Berton, J. Tittmann, F. Hennrich, M. M. Kappes and M. Mayor, *Macromolecules*, 2012, **45**, 713–722.

65 J. Gao, M. Kwak, J. Wildeman, A. Herrmann and M. A. Loi, *Carbon*, 2011, **49**, 333–338.

66 H. Ozawa, T. Fujigaya, Y. Niidome, N. Hotta, M. Fujiki and N. Nakashima, *J. Am. Chem. Soc.*, 2011, **133**, 2651–2657.

67 K. S. Mistry, B. A. Larsen and J. L. Blackburn, *ACS Nano*, 2013, **7**, 2231–2239.

68 B. J. Landi, H. F. Ruf, C. M. Evans, C. D. Cress and R. P. Raffaelle, *J. Phys. Chem. B*, 2005, **109**, 9952–9965.

69 N. Berton, F. Lemasson, F. Hennrich, M. M. Kappes and M. Mayor, *Chem. Commun.*, 2012, **48**, 2516–2518.

70 H. Park, A. Afzali, S.-J. Han, G. S. Tulevski, A. D. Franklin, J. Tersoff, J. B. Hannon and W. Haensch, *Nat. Nanotechnol.*, 2012, **7**, 787–791.

71 L. S. Liyanage, H. Lee, N. Patil, S. Park, S. Mitra, Z. Bao and H.-S. P. Wong, *ACS Nano*, 2012, **6**, 451–458.

72 B. K. Sarker, S. Shekhar and S. I. Khondaker, *ACS Nano*, 2011, **5**, 6297–6305.